MULTIFREQUENCY ACOUSTIC EMISSIONS (*AE*) FOR MONITORING THE TIME EVOLUTION OF MICROPROCESSES WITHIN SOLIDS

Gabriele Paparo and Giovanni P. Gregori

Istituto di Acustica "O. M. Corbino", CNR, via Fosso del Cavaliere 100, 00133 Roma (Italy)

ABSTRACT. Microprocesses occur like chain reactions where bonds progressively yield. The temporal evolution can be tracked by multifrequency *AE*. Two principle ideas. One relies on time series of *AE* of increasingly lower frequency. The second compares time histories of every *AE* event (fixed frequency) with a lognormal distribution: deviations reveal additional parameters, and the tail results modulated by external effects, envisaging what triggers every *AE*. Natural environmental phenomena are effective feasibility tests, for subsequent laboratory implementation.

INTRODUCTION

Microprocesses within solids occur like chain reactions, by which molecular and/or atomic bonds progressively yield. The temporal evolution of such occurrence can be tracked in some detail by suitable data handling of multifrequency acoustic emission (*AE*) monitoring. This can be achieved according to two principle ideas. One relies upon consideration of the time series of different *AE* signals of increasingly lower frequency, corresponding to the yield of increasingly larger pores and/or structures. The second criterion considers the specific time history of every *AE* event, at every given and fixed frequency, in terms of comparison with a distribution that, as a first order approximation, ought to be lognormal. Deviations from such model reveal hidden degrees of freedom (*d.o.f.*), envisaging remarkable heuristic potentialities. Moreover, the tail of such distribution eventually results modulated by some applied external effects, resulting into a tool for envisaging, whenever needed, what cause that triggered every given *AE* release. Some phenomena observed in the natural environment are expressive case histories for testing the feasibility of such approach, to be later suitably implemented also within the laboratory.

Time Series of *AE* of Decreasing Frequency

Minor pores, or crystal defects, or flaws, yield first, and release comparatively higher frequency *AE*. They coalesce into progressively larger pores or flaws, while releasing *AE* of progressively lower frequency. Whenever such frequency is as low as

CP657, *Review of Quantitative Nondestructive Evaluation Vol. 22,* ed. by D. O. Thompson and D. E. Chimenti

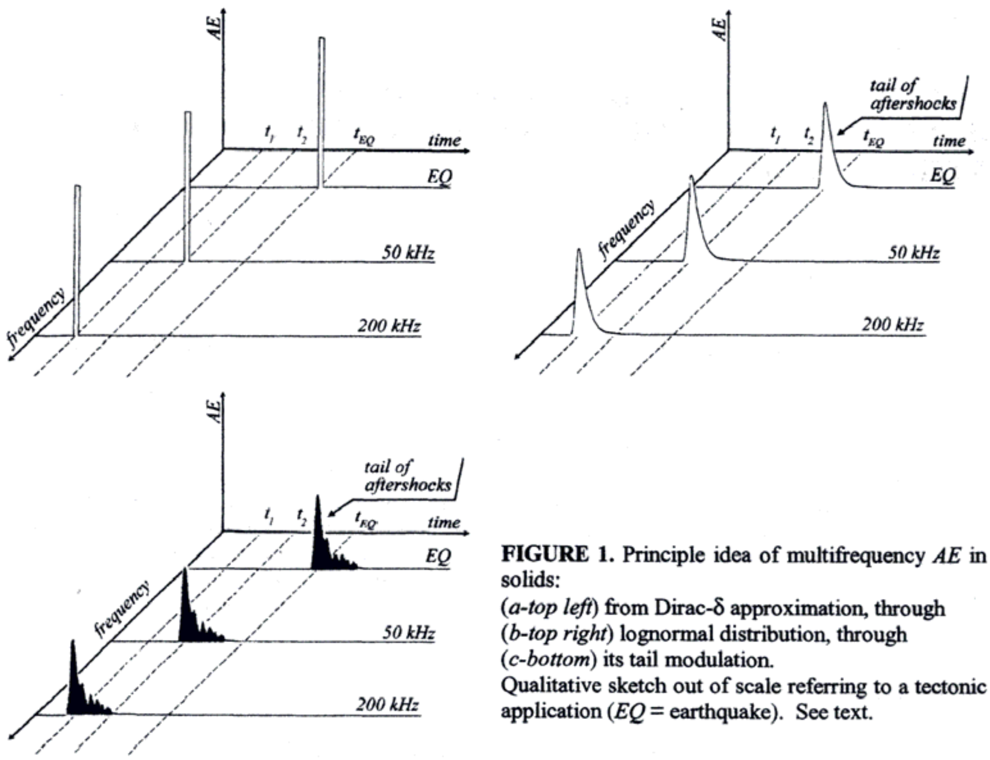

FIGURE 1. Principle idea of multifrequency *AE* in solids:
(*a-top left*) from Dirac-δ approximation, through
(*b-top right*) lognormal distribution, through
(*c-bottom*) its tail modulation.
Qualitative sketch out of scale referring to a tectonic application (*EQ* = earthquake). See text.

~0.5 ÷ 1. Hz, the large-scale mechanical structure yields, and (e.g. in the case of a tectonic structure) a landslide or an earthquake is triggered.

A key physical distinction depends on whether the space distribution is 3D or 2D of the prime *AE* sources. The 3D case history occurs e.g. whenever some hot fluid penetrates at some high pressure into the pores of the solid sample, and makes some bond to yield. In such case, all *AE* events appear uncorrelated with each other, because the prime cause, i.e. fluid diffusion into the pores, is random, and no pore can keep memory of what pores already yielded. Instead, the 2D case typically occurs when a crystal breaks along a cleavage, by which every bond yields, while it keeps memory of the fact that its close-by bonds already yielded along some preferential plane (i.e. along the plane where such bonds are comparatively weaker).

When comparing such two typical 3D *vs.* 2D occurrences, the *AE* time series display a completely different trend. A most effective and simple algorithm for detecting such different behavior is the *box counting method* to be applied to the *AE* time series. Such algorithm is a well-known elementary item in fractal analysis [1]. 3D case histories do give a fractal dimension $D=1$. In contrast, when the system tends to become progressively better ordered in space, the *AE* result progressively organized, and D progressively decreases towards $D=0$. (the null value is attained only whenever the entire *AE* time series is concentrated at one time instant, at which instant all events simultaneously occur; differently stated, this is the case of maximum reciprocal memory between all *AE* events). The application of such method to *AE* monitoring in geophysics, upon distinguishing different tectonic settings, was discussed elsewhere and is not here repeated (see [2,3,4]).

As far as laboratory applications are concerned, we recall an experiment carried out by several identical elastic bars, composed of a special alloy [5]. Whenever the bar was bent for the first time, they gave *D=1*. Every subsequent bending revealed decreasing *D*, being (roughly) $D \sim 0.9$ during the second bending, $D \sim 0.8$ during the third bending, etc., due to the fact that, during every bending, some minor amount of bonds always yield, because no ideally perfect elastic material exists. Moreover, such yielding occurs along progressively better-organized patterns, or cleavage planes, between the micro-crystals of the alloy. The decrease of *D*, however, is to be stopped whenever the alloy attains some final saturation internal state, after which the fatigue of the material ought to be investigated.

Time History During Every *AE* Event

A first-order description of every *AE* event can be given as a Dirac δ - function (Figure 1a), by which it is assumed that, at every time instant during the process, the *entire* set of pores or flaws simultaneously shares the identical trend *vs.* time. Instead, consider that comparatively larger pores or flaws do release (as mentioned above) comparatively lower frequency *AE*, while several simultaneously occurring and comparatively smaller pores or flaws are *still* releasing higher frequency *AE*. This implies that the former Dirac δ - function must be improved, and substituted by a suitable lognormal distribution. Such inference can be motivated by the classical argument of the *Kapteyn class* distributions. Since textbooks only seldom report such algorithm, a concise remind is given in the next section

Its rationale is much similar to the case of the investigation either of the user distribution of a public service (this is the logical motivation for the rush-hour effect), or of the hypsometric curve (i.e. the distribution of topographic heights with respect to a reference surface, e.g. considering the surface of a heap of coal, or of a planet, etc.; every particle of matter can be located at a given height only because some other particles support it underneath). The process can be depicted in terms of the aforementioned reaction-chain (atomic bonds preferentially yield where some other atomic bond already yielded). This is in fact observed e.g. in the laboratory. This is clearly shown, e.g., by a figure in [6], dealing with tests on *7050-* and *7075-T7351 Al* alloys, which differ only by number and size of inclusion. Measurements were carried out on specimens cut in different parts of an alloy slab. They applied two different smoothing procedures, by which the need is stressed for adequate filtering of the lesser temporal details, for achieving clear evidence of the aforementioned expected statistical features of the process. Moreover, in this same respect, an investigation on the form of the distribution of the *AE* release *vs.* time, carried out independent of the aforementioned rationale, revealed that the distribution definitely appears lognormal, and never e.g. a Weibull distribution [7].

A second order description of the multifrequency *AE* release is therefore in terms of lognormal distributions (Figure 1b), where, in the case of a tectonic application, the lognormal tail can be identified in the earthquake frequency range with the well-known classical aftershocks.

Kapteyn Class Distributions and the P*robit Diagram*

The present brief mentions are borrowed from [8], while the original formulation is by Kapteyn and van Uven [9]. A variate x is known in terms of a set of observations $\{x_j\}$ ($j=1,2, ...,$N). Pre-choose a given interval Δx and call $N(x)$ the number of x_j that fall within the interval between x and $x+\Delta x$, while the associated *frequency* is $N(x)$/N. The concept of *continuous distribution* permits the transition from a *discrete* description of such *frequency*, in terms of finite increments Δx, into a *continuous* function $\varphi(x)$ called *probability density*. Hence, $\varphi(x)dx$ is the *probability* that a given x_j occurs between x and $x+dx$. Recall that

$$\int_{-\infty}^{+\infty}\varphi(x)dx = 1 \qquad \Phi(x) = \int_{-\infty}^{x}\varphi(z)dz \qquad \Phi(+\infty) = 1 \tag{1}$$

where $\Phi(x)$ is the *integral distribution*. Call $y = G(x)$ a function with $-\infty < y < +\infty$, $a \leq x \leq b$, $-\infty \leq b \leq +\infty$ and suppose that $G'(x)$ is defined for all x in the interval of definition. Assume that y has a normal distribution, hence x has the distribution

$$d\Phi(x) = \varphi(x)dx = d\Psi\left(\frac{G(x)-\mu}{\sigma}\right) = \frac{1}{\sqrt{2\pi}\sigma}exp\left[-\frac{1}{2\sigma^2}(G(x)-\mu)^2\right]\left|\frac{dG(x)}{dx}\right|dx \tag{2}$$

and the average and standard deviation of $G(x)$ are, respectively,

$$\mathcal{M}\{G(x)\} = \mu \qquad \sigma\{G(x)\} = \sigma \tag{3}$$

Kapteyn (*ibid.*) deduced a whole class of distributions from the normal by means of the following argument. Suppose that x does not result from the sum of a large number of variates, rather that it depends on a large number of causes, every one giving one successive "impulse", the effect of which depends partly on the intensity of the "impulse" itself, and partly on the magnitude of x prior to the occurrence of such an "impulse". Let $\{z_j\}$ $(j=1,2, \ldots,\boldsymbol{Z})$ be a time-series of independent impulses originated by a number $\boldsymbol{C}$ of causes, and call x_i the result of the first i such impulses. Then, assume that x_{i+1} depends only on the value of x_i and not on the previous history of the system. Hence, assume that there exists a function $g(x)$ such that

$$x_{i+1} = x_i + z_{i+1}g(x_i) \qquad g(x) \neq 0 \tag{4}$$

If $\boldsymbol{C}$ is large, and therefore every impulse gives a small contribution, it is

$$\sum_{j=1}^{C} z_j = \sum_{i=0}^{C-1}\frac{x_{i+1}-x_i}{g(x_i)} \approx \int_{x_0}^{x}\frac{dx}{g(x)} = G(x) \tag{5}$$

Owing to the central limit theorem, it is reasonable to guess that $G(x)$ has a normal distribution; hence, x has the distribution (2). One particular case history occurs whenever $g(x) = x$, which is the aforementioned rush-hour concern in a public service, by which

$$\int\frac{dx}{x} = \ln x \tag{6}$$

and the *lognormal* distribution is thus obtained

$$d\Phi(x) = \varphi(x)dx = d\Psi\left(\frac{ln\,x-\mu}{\sigma}\right) = \frac{1}{\sqrt{2\pi}\sigma}exp\left[-\frac{(ln\,x-\mu)^2}{2\sigma^2}\right]\frac{dx}{x} \qquad 0 \leq x < \infty \tag{7}$$

$$\mathcal{M}\{\ln x\} = \mu \qquad\qquad \sigma\{\ln x\} = \sigma \tag{8}$$

where the symbols ψ and Ψ are sometimes used instead of φ and Φ, respectively, whenever it is emphasized that the distribution is normalized in such a way that $\mu = 0$ and $\sigma = 1$. Kapteyn's class distributions can be effectively dealt with by considering that the function $u=\Psi(t)$ for the whole interval $-\infty < t < +\infty$ is always increasing. Hence, it is possible to reverse it and define a function (prior to computer age there was need for numerical values available from the classical tables by Fisher and Yates)

$$t = \Psi^{-1}(u) \tag{9}$$

In the case of a normal distribution, this amounts to compute

$$u = \Psi\left(\frac{t-\mu}{\sigma}\right) \qquad \Psi^{-1}(u) = \frac{t-\mu}{\sigma} = \mathrm{v}_1(t) \qquad \mathrm{v}_2(t) = \Psi^{-1}(F(t)) \qquad \mathrm{F(t)} = \frac{\mathrm{N(t)}}{N} \tag{10}$$

where $\mathrm{v}_1(t)$ and $\mathrm{v}_2(t)$ refer to the theoretical and observed curve, respectively. Such plot of either $\mathrm{v}_1(t)$ and/or $\mathrm{v}_2(t)$ *vs.* t is called *probit diagram*. In the case of a normal distribution, it is a line through the point (μ , 0) with slope $1/\sigma$ and it can be intuitively depicted as a mathematical way of stretching the sigmoid into a straight line. In the case that $G(x)$, rather than x, has a normal distribution, the two quantities

$$\mathrm{v}_1 = \frac{G(t)-\mu}{\sigma} \qquad\qquad \mathrm{v}_2(t) = \Psi^{-1}(F(t)) \tag{11}$$

ought to lie very close to each other. Such entire algorithm is thus an expressive way of carrying out a visual test of the Gaussianicity of a given distribution (although for such purpose other methods can be effectively applied, which do not need for drawing a plot and deciding by visual inspection).

A feature of the *probit diagram* is that, compared to the straight-line $t = \mu$, the statistical fluctuations become stronger close to its ends. This is because

$$\sigma^2\{\Psi^{-1}(F(t))\} \approx \frac{1}{\psi^2(\mathrm{v})} \frac{\Psi(\mathrm{v})(1-\Psi(\mathrm{v}))}{n} \xrightarrow[|\mathrm{v}| \to \infty]{} \infty \qquad \mathrm{v} = \frac{t-\mu}{\sigma} \tag{12}$$

Another example borrowed from [8] deals with *750* electricity consumers, whose consumption is measured in hours t of use corresponding to maximum load (Δt = *100 hours*). This is a clear example of lognormal distribution.

Hidden Degrees of Freedom

The reaction chain concept is simple and expressive, though certainly physically approximate. One can therefore effectively apply the *probit diagram* technique, by which a perfect, lognormal, distribution provides exactly a linear trend. Instead, suppose that such linearity is observed only at a first order approximation. One can introduce some correcting parameters, depicted e.g. by means of a polynomial trend in the *probit diagram*, which appears just like some minor deviation compared to the first order ideal merely linear trend. Or, on can use an exponential function, or other. Such improved curve, compared to the linear trend, depends on a few additional *d.o.f.* We do not know their actual physical meaning, though we know that they exist, that they are physically significant, that the *probit diagram*, which is a well-defined precise algorithm, can derive them in a unique way. Differently stated, we are able to evaluate them quantitatively and monitor their time evolution. This results into an effective algorithm for investigating how many *d.o.f.* are needed for describing our system, according to the precision and sensitivity of our measurements, and for computing an actual set of their observed values.

External Modulation of the Tail of the Distribution

Sometimes it is difficult to associate with each other the *AE* events recorded at different frequencies, or equivalently, to associate a given trigger to every observed *AE* record at every given frequency. In the laboratory, where the triggering stress is known, this may appear obvious. However, under more general conditions (such as e.g. when monitoring within the environment), arbitrariness can sometimes imply non-univocal interpretation, with an eventual severe drawback on the final interpretation. Under such more general and difficult circumstances, some external modulation that controls the system can result very helpful.

For instance, in the case of a natural structure, it is known that the Earth's tide causes a periodical and approximately daily wave of upheaval and subsidence of the entire structure, by which the endogenous fluids, the pressure of which is responsible for producing the pore yield, do afford in escaping more or less freely, depending on the temporal variation of the overlying weight of the Earth's layers, which are a real lid for them.

Such additional effect can again be depicted in terms of lognormal distributions that display a superposed tidal modulation, the amplitude of which is approximately *constant* every day, though in terms of its *percent* variation of the actual amplitude of the lognormal distribution. Hence, the *absolute* amplitude of such tidal variation must be expected to *decrease* every day, depending on the decrease of the non-modulated former lognormal tail (Figure 1c). We also note that, in general, the phase of such tidal modulation is different *vs.* local time, depending on the date and on the very complex lunar orbit. In particular, in such third case history, the aftershock frequency of an earthquake ought to be likened to a (speculated and, in principle, expected) minor diurnal modulation (of tidal origin) of the time distribution of aftershocks. Figure 2 contains a set of a few such examples borrowed from a few geophysical observations. The inhabitants of the Orchi site frequently listen acoustic noise originated underground.

As far as the laboratory applications are concerned, the leading principle remains the same, though the space- and time-scales in general are quite different. For instance, in the Vesuvius case history, by means of such criterion we were able to infer that one such expected lognormal distribution has a typical tail lasting several days, and this can be most easily evidenced by the such almost diurnal tidal modulation of the tail (in fact, according to our present understanding of volcanoes, our knowledge permits no realistically reliable inference; we obtained such evidence observationally, i.e. by means of such tail modulation argument). Obviously, such rationale can be applied provided that the system (i.e. Vesuvius) is not subject to prime triggers occurring in a time sequence with time lags shorter than the modulation period (i.e. than a few days). In contrast, in the case of a laboratory experiment carried out on a known sample and by means of a known trigger, the typical tail duration will be substantially shorter (such as e.g. in the aforementioned test on two *Al* alloys). The external applied modulation of the tail ought to be accordingly conceived, resulting into an effective mean for detecting the response times of the material to some applied stress.

The purpose of the present paper is in envisaging such possibility, and in showing how the principle idea can effectively work, at least when considering some intriguing case histories that can be found within the natural laboratory of the environment.

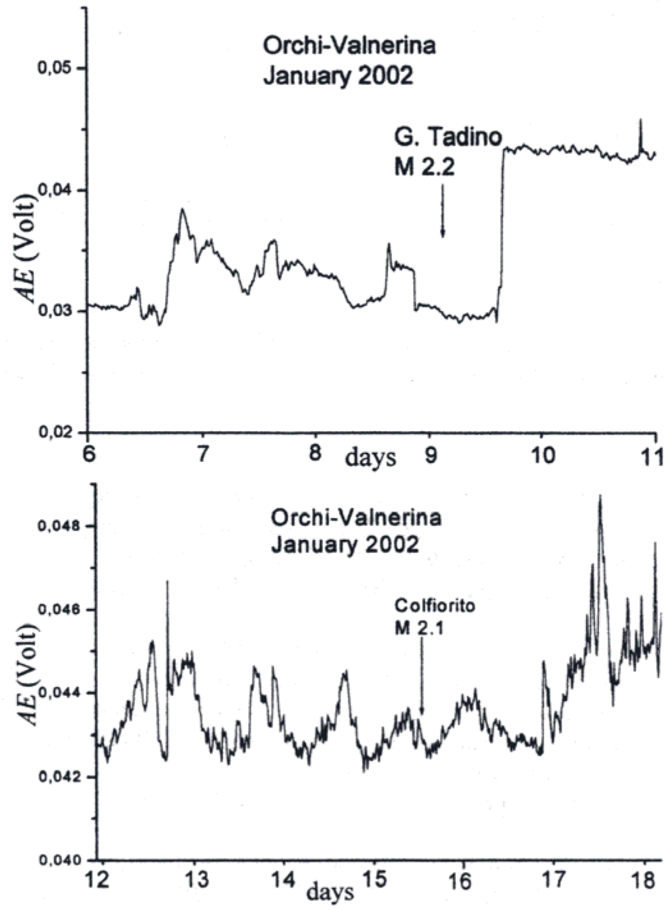

FIGURE 2a. Examples of tidal modulation of the tail of the lognormal distribution for *AE* recorded in a seismic area in central Italy (Umbria). Earthquake occurrence and respective magnitude are indicated. See text.

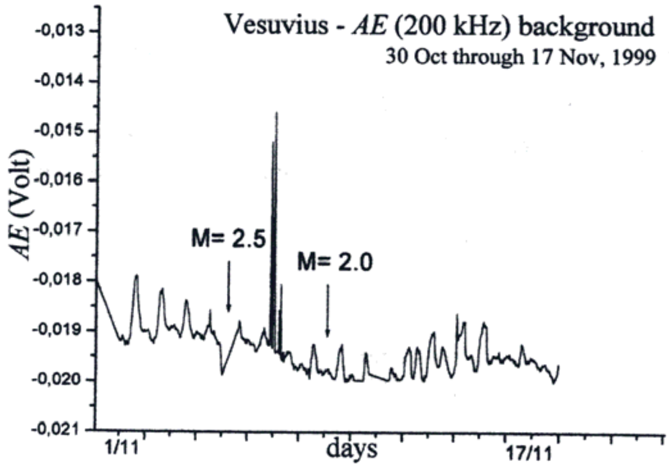

FIGURE 2b. Example of tidal modulation of the tail of the lognormal distribution for *AE* recorded on Vesuvius. Earthquake occurrence and respective magnitude are indicated. See text.

ACKNOWLEDGEMENTS

We are indebted with Professor I. Marson and with U. Coppa for relevant discussions, and with R. de Ritis and A. Taloni for data handling on related items.

REFERENCES

1. For instance, Turcotte, D. L, *Fractals and chaos in geology and geophysics*. Cambridge Univ. Press, 1992, 221 pp. The general logical strategy is discussed by Gregori, G. P., 1998. *Annali di Geofisica*, **41**, (5/6), pp. 767-786.
2. Paparo, G., Gregori G. P., Coppa U., de Ritis R., and Taloni A., *Annali di Geofisica* (in press), (2002).
3. Gregori, G. P., Paparo G., Coppa U., and Marson I., 2001 "Acoustic Emission (*AE*) in geophysics", in *Actas E-GLEA2, Segundo Encuentro Latinoamericano de Emisìon Acùstica, Primero Iberoamericano*, edited by M. I. Lòpez Pumarega and J. E. Ruzzante, Grupo Latino Americano de Emisìon Acùstica. 1650 General San Martin (prov. Buenos Aires, Argentina), pp. 57-78 (2001).
4. Gregori, G. P., Paparo G., Coppa U., and Marson I., *Boll. Geofis. Teor. Appl.*, (in press), (2002).
5. Braccini, S., Casciano C., Cordero F., Fiasconi F., Gregori G. P., Majorana E., Paparo G., Passaquieti R., Puppo P., Rapagnani P., and Ricci F., *Phys. Lett. A* (in press) (2002).
6. Scott, Ian G., *Basic acoustic emission*, Gordon and Breach Science Publishers, New York, etc., 1991, 246 pp., who borrowed it from Cousland, S. McK., and Scala, C. M., *Metal Sci.*, **15**, p. 609, (1983).
7. Lòpez Pumarega, M. I., Piotrkowski, R., and Ruzzante J. E., *J. Acoust. Emis.*, **17**, (1-2), pp. 61-68, (1999).
8. Arley, N., and Buch K. R., *Introduction to the theory of probability and statistics*, J. Wiley & sons, Inc., New York, 1950, p. 240.
9. Kapteyn, J. C., and van Uven M. J., *Skew frequency-curves in biology and statistics*, Groningen, p. 69 (1916).